Surprising Behavior During Dissipation and Collision of Flexural Waves in Carbon Nanotubes

Surprising Behavior During Dissipation and Collision of Flexural Waves in Carbon Nanotubes

Venkata Rajesh Saranam and P. Alex Greaney[1]

School of Mechanical, Industrial, & Manufacturing Engineering
Oregon State University
Corvallis, OR 97331

Abstract: The manuscript reports on simulations of the intrinsic dissipation of standing and traveling flexural vibrations in carbon nanotubes. It is found that extended traveling and standing waves exhibit anomalous dissipation, during which the excited modes experience massive damping that is triggered by the accumulation of energy in special gateway modes. In the second part of this work the attenuation of traveling flexural wave packets is examined—including the collisions between wave packets. Surprisingly, these wave packets show markedly different dissipation behavior from extended waves with the same wavelength and amplitude. Moreover, the wave packet collisions are seen to be sensitive to the direction of collision, hinting at temperature gradient induced reduction of the thermal conductivity. Following the cascade of energy as it dissipates it is seen that scattering of energy into other flexural modes has little effect on the net energy flux, while dissipation into non-flexural modes is thermally resistive.

1 Introduction

Carbon nanotubes (CNTs) with their superior mechanical [1, 2], electrical [3], and thermal properties [1, 4] and their accompanying large aspect ratio and low density, have revolutionized nanotechnology industries. CNTs' remarkable stiffness and low density can result in mechanical vibrations with frequencies reaching the 10 GHz range. Moreover, these vibrations can be driven and sensed electronically [5, 6, 7, 8, 9] makes them a seemingly ideal candidate for chemical and mass sensing [10]. Coupling high-frequency mechanical oscillations to field emission also opens CNTs to wireless communications applications.

A fundamental limitation of CNT resonators are their poor quality factor Q (2π times the inverse fraction of energy dissipated per cycle). Although Q factors of 10^5 have been observed experimentally in defect-free CNTs at milli-kelvin temperature [9], at ambient temperature Q falls to a few hundred. Simulations of ring-down in short CNTs exhibited transient anomalous dissipation in which Q drops close to 10 for a few picoseconds and then recovers [11]. The waiting time for the anomalous dissipation is dependent on the initial excitation energy. An effect analogous to the Mpemba effect is observed in which larger initial excitations take less time to dissipate [12]. It was found that rapid dissipation is triggered by the accumulation of energy in specific modes called gateway modes. Anomalous dissipation occurs due to small excitation of the gateway mode causing strong anharmonic coupling to the excited mode. The result is that once this coupling is activated, the excited mode rapidly dissipates energy into the gateway mode and other low frequency modes. The excited and low temperature modes come quickly into local thermal equilibrium and the rapid dissipation slows, with further dissipation limited by the rate of energy loss into high frequency

[1]Corresponding author: alex.greaney@oregonstate.edu

modes. The mechanism is described in more detail by Greaney *et.al.*[12]. This prior research suggests that if one can control the energy accumulation in gateway modes then one can tune the damping of CNT resonators, opening applications for thermal switching or mechanical signal processing. The objective of this work is to determine if there is an experimentally observable manifestation of this anomalous dissipation in large-scale systems. Towards that end, this work examines the dissipation in very long CNTs, and extends the study of dissipation to include the attenuation of traveling wave packets, and wave packet collisions with their counterpart gateway modes. After describing the simulation setup the first part of this manuscript focuses on dissipation mechanisms for delocalized standing and traveling waves, and identifies participating gateway modes. The latter part of the manuscript describes dissipation of traveling wavepackets and the collisions between wave packets.

2 Methods

Dissipation was studied in (10,0) CNTs using molecular dynamics in which the interatomic potentials are modeled with the AIREBO potential [13] (as implemented in LAMMPS [14]). The AIREBO potential includes anharmonic interactions between carbon atoms, and long-range dispersion forces. This potential is widely used for modeling carbon nanostructures, and has been validated for simulating mechanics of CNTs and in particular anharmonic interactions in CNTs [15]. Sections of tube 83.7 nm long were simulated with periodic boundary conditions applied along the tubes' axis. This corresponds to 200 repeat units of the (10,0) tube (8000 atoms). These simulated tubes are ten times longer than those in prior simulations in which anomalous dissipation was first observed [11] and thus enabled the participation of many more long wavelength low-frequency modes in the dissipation process. In the studies of dissipation in short CNTs the anomalous dissipation was found to occur in tubes with other diameters, chiralities, and was also independent of our choice of interatomic potential. Thus, in this work we restrict our simulations of these very large systems to just (10,0) tubes, confident that their behavior is representative of all tubes.

A typical simulation proceeded as follows: (1) The atomic coordinates and the periodic repeat length of the simulation cell were optimized. (2) The CNT was heated in the canonical ensemble over 100 ps to a temperature T_b (called the background temperature) using the Noise-Hoover thermostat. (3) The thermostat was then turned off and simulated in the micro-canonical ensemble for 100 ps to permit the energy to equilibriate across the full vibrational spectrum of the CNT. (4) A vibration was then excited by adding potential and kinetic energy to selected phonon modes raising the temperature of the whole tube by ΔT_{ex}. (5) The excited tube was then simulated in the microcanonical ensemble for at least 100 ps during which the energy in the flexural modes of the tube was determined using mode projection. For each simulation, integration of the system's phase space trajectory was performed using the velocity Verlet algorithm with a time step of 0.2 fs which was sufficient to reduce fluctuations in the total energy of the microcanonical ensemble to less than 10^{-5} of the mean kinetic energy.

The vibrational modes of the CNT with wave vector k were computed by finding the complex eigenvectors of the tube's dynamical matrix, $D(k)$. The dynamical matrix was constructed including stiffness contributions between atoms up to 1.6 nm apart. The dispersion relation for a (10,0) CNT has 120 branches—the first few low-frequency branches are plotted in Fig.1, with the flexural branch

plotted in blue. At each k value commensurate with the 200 repeat unit tube the two degenerate flexural modes were found and used to construct a flexural mode with principle displacements along the y-direction, as show in Fig.1. These modes are complex, with the atomic displacement given by the real part and the velocity given by the imaginary part.

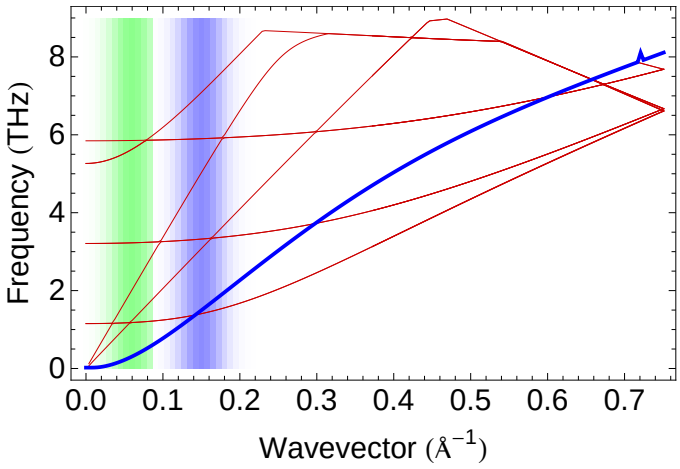

Figure 1: *Low frequency portion of the phonon dispersion in a (10,0) AIREBO carbon nanotube.There are 120 branches in total and the branch for the flexural modes is highlighted in blue. The vertical blue shaded stripe indicates the weighting of the modes used to construct the wave packets with a wavelength of 1/20th or the tube length. The green stripe shows the weighting used to construct the gateway wave packet.*

Three types of vibration were excited: standing waves, traveling waves, and wave packets. Standing waves were single flexural modes delocalized over the entire length of the tube. These are excited by adding instantaneous velocity to the system along the imaginary part of the mode's eigenvector. Traveling waves are also delocalized single wavelength modes, and were constructed adding instantaneous displacements in addition to an instantaneous velocity. While the eigenvectors give the direction around equilibrium, the modes' trajectories are significantly curved involving local rotation of the tube's axis. Thus, the initial displacement for the traveling wave was obtained from the first apogee displacement of the standing wave. This procedure resulted in traveling waves with less than 2% difference between potential and kinetic energy. A similar procedure was used to construct the initial displacement vector of the wave packets. Wave packets are localized vibrations constructed from the superposition of flexural modes weighted by a gaussian about the central wave vector k.

To make the comparison with the earlier work we focused our attention on wavelength 4.2 nm (*i.e.,* 1/20th of the box length, or 10 repeat units). For the wave packets, the green and blue shaded bands in Fig. 1 indicate the gaussian weighting of modes used to construct the wave packets. These resulted in wave packets approximately 40 nm wide (roughly one fifth of the length of the tube). Delocalized modes were excited with either 0.4625 meV/atom or 0.925 meV/atom (raising the temperature of the entire tube by 14.3 and 28.6 K respectively). This enabled comparison of the damping of a standing wave with the dissipation of traveling waves with the same total energy, and with the same displacement. The ring-down of the excited mode was tracked by projecting the atomic velocity on to the eigenmodes of the tube. The results shown for each temperature are the average of at least eight simulations from equilibrated data files.

A background temperature (T_b) of range 0–500 K in steps of 50 K was chosen. In these simulations our aim was to observe energy dissipation mechanisms during collisions of flexural phonon modes. The simulations were conducted at temperatures well below the Debye temperature where the high frequency modes would not be occupied. This approach is justified in two ways: first, the simulations are not of a system at thermal equilibrium, but the relaxation of a system towards equilibrium. Second, prior work showed that the high-frequency modes do not participate in the dissipation [12]. Simulations at higher temperature show the same qualitative behavior, but at lower temperature one can more easily follow the energy through the other modes of the tube as it dissipates.

3 Standing and traveling waves

Figure 2 shows the ring-down of the mean kinetic energy in the excited flexural mode for a standing wave of initial energy 0.925 meV/atom (a), a traveling wave with the same total energy (b) and a traveling wave with the same maximum amplitude (*i.e.* total energy of 14.8 meV/atom) (c). In each plot the ringdown of the kinetic energy at temperatures ranging from 0–500 K is shown. For each case the ring-down shows strong anomalous dissipation similar to the case for short tubes reported earlier [11]. At low temperatures the ring-down shows a long region of very little dissipation which transitions abruptly into a period of strong dissipation for 10–20 ps during which the mode loses about 70% of its initial excited energy. Increasing the background temperature T_b decreases the time for the onset of anomalous dissipation, reduces the severity of anomalous dissipation and increases the extent of energy lost in the excited flexural mode.

The dissipative behavior of the standing wave most closely resembled the dissipation of the travelling wave with same total energy. This is surprising, because the maximum amplitude is $\sim 1/\sqrt{2}$ times smaller than the standing wave, and thus the effect of anharmonicity should be smaller. The traveling wave with same amplitude in Fig.2(c) showed a reduction in waiting time before anomalous dissipation, suggesting the anomalous dissipation in a SWCNT cannot be explained by anharmonic coupling alone.

While the overall ring-down behavior in these long tubes closely resembled the prior simulations for shorter tubes, three significant differences were observed: the system used a different gateway mode, the dissipation was spatially localized, and the dissipation showed pronounced recovery or rebound.

Anomalous dissipation is triggered by the accumulation of energy in few special low frequency flexural modes that we term gateway modes. The importance of excitation of this mode for triggering rapid dissipation was established by observing that when the gateway mode was excited externally, anomalous dissipation began immediately. In these simulations of long tubes the gateway mode was the flexural mode with wavelength 10.4 nm (*i.e.*, width one eighth of the computational cell). This mode was not commensurate with the periodic boundaries of the shorter systems simulated previously. The energy in the gateway mode during ringdown of the traveling wave is plotted in Fig.2(d). Dissipated energy went into the gateway mode and other propagating low frequency (long wavelength) flexural modes with the rest going into other non-flexural modes. The combined energy in all of the low frequency flexural modes (with wavelengths up to 27.7 nm) closely tracked the instantaneous heat flux. This indicates that while dissipation from the initially excited traveling wave occurs, only dissipation to non-flexural modes is thermally resistive.

In each of the plots in Fig.2(a–c) the energy of the excited mode showed a pronounced rebound

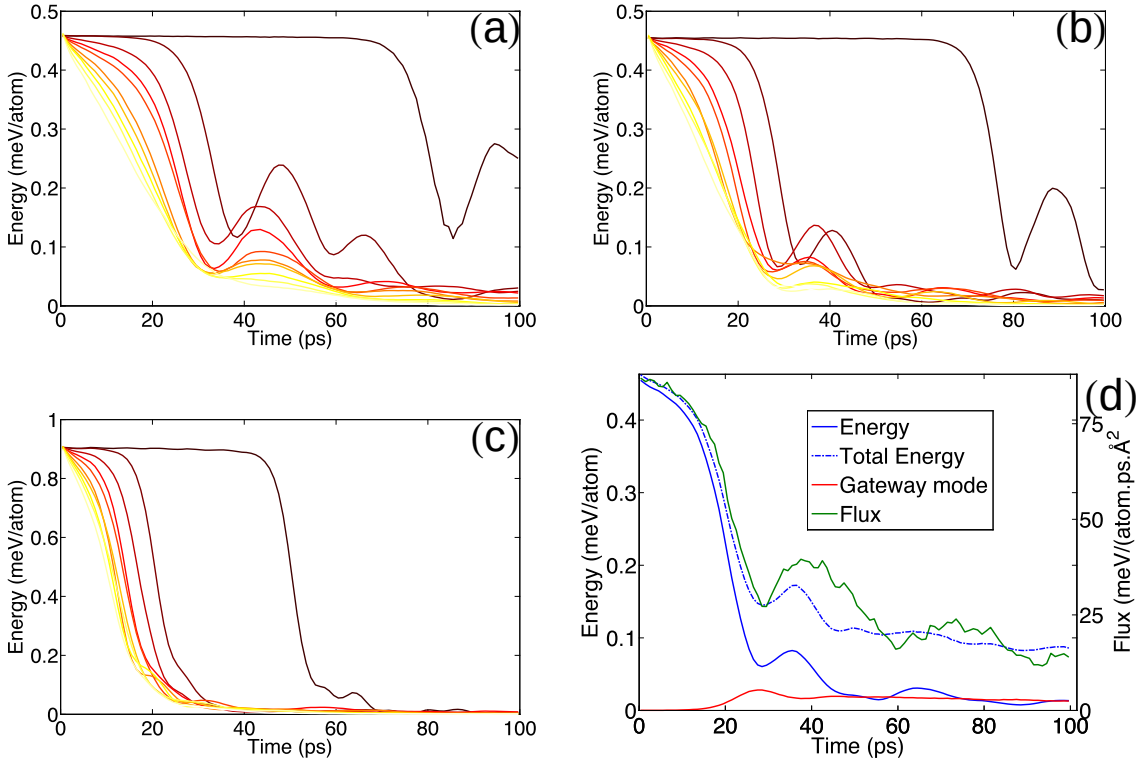

Figure 2: *Ring-down of flexural mode with background temperature of 0(brown), 5, 50, 100, 150, 200, 250, 300, 350, 400 and 500 K (yellow) for: (a) standing waves with 0.925 meV/atom, (b) traveling waves with same total enegy (and therefore a smaller amplitude), (c) traveling waves with same amplitude, and (d) flux and energy plot for traveling wave same kinetic energy at T_b = 100 K.*

after the period of severe damping. This rebound suggests a beating energy exchange with a modes nearby in frequency in addition to dissipation to high frequency modes.

The spatial distribution of energy during dissipation was observed by mapping the kinetic energy along the tube length over the course of the simulation (Fig.3). These maps reveal some important insights into the dissipation sequence. The kinetic energy map from one (representative) simulation of a standing wave (with T_b = 100 K) is given in Fig.3(a), and shows that the energy remained delocalized over the entire tube during anomalous dissipation. Similarly, mapping the energy for the traveling wave resulted in diagonal stripes as the wave is traveling. To make it easier to interpret, the map was sheared in time so as to transform it into a moving frame of reference. The shearing strain is related to the velocity of the reference frame and enabled us to visually measure the velocity of the traveling wave (and its dissipation products) in the same way that a strobe can be used to visually measure the frequency of very high-frequency motion. Sweeping the image shear from zero upwards, the velocity was noted every time wave patterns emerge that are stationary with respect to the moving reference frame. Fig.3(b) shows the kinetic energy map for a typical traveling wave (again with $T_b = 100$ K) in a reference frame moving with velocity 6300 ms^{-1}, *i.e.*, at the speed of the traveling wave. Anomalous dissipation occurred after approximately 43 ps. It is clear that the dissipation was not delocalized and resulted in a local hot spot in the moving reference frame—that is, a localized but traveling wave packet or pulse. Figs.3(c)&(d) show the same energy map sheared

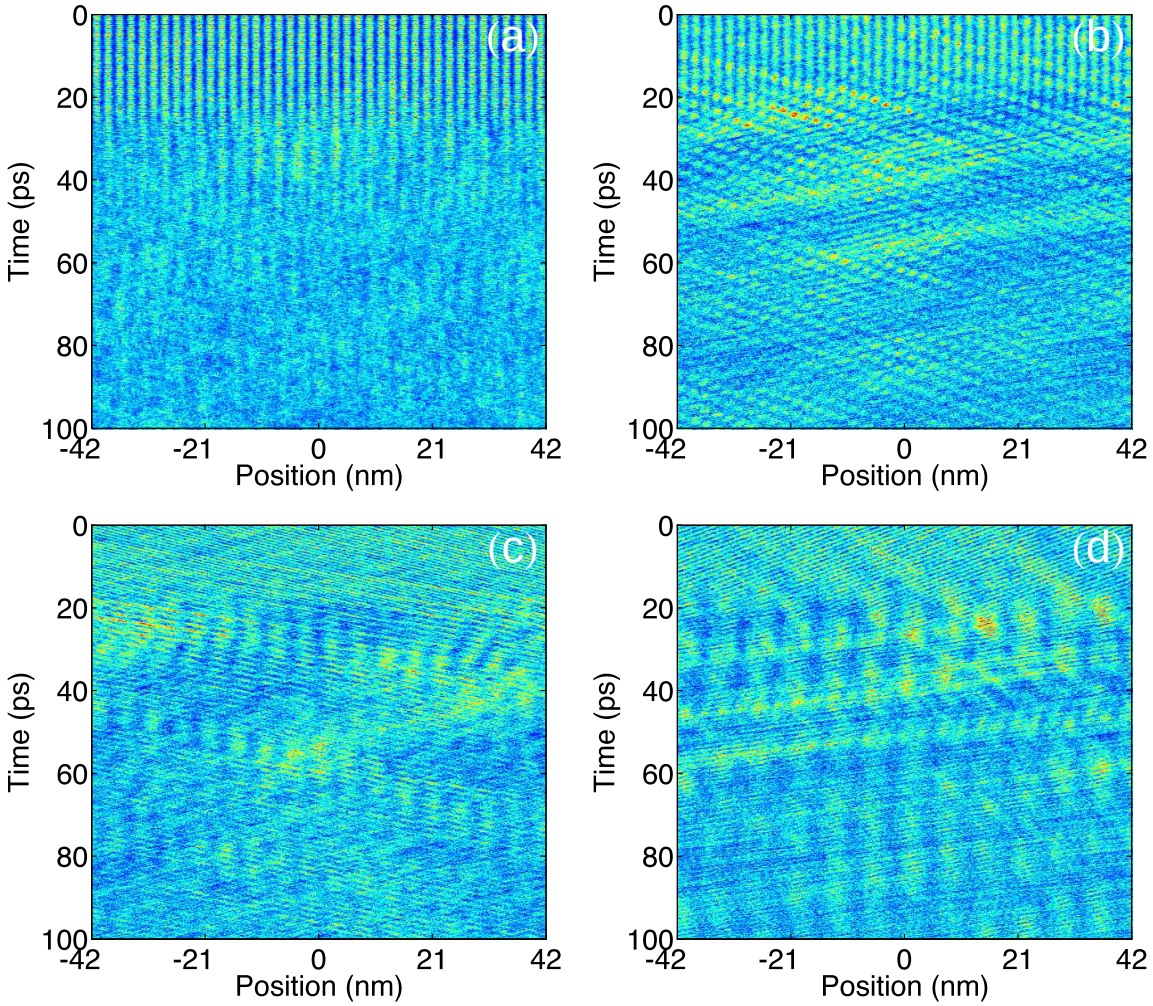

Figure 3: *Maps showing the evolution of the kinetic energy along the tube's length during a typical simulation. The simulations were performed with T_b = 100 K. Map (a) is for a standing wave with excited to 0.925 meV/atom. Maps (b–d) are for a traveling wave with the same energy. Plots (b–d) have been sheared into the moving reference frame with velocities of 6300, 3330, and 8330, ms^{-1} respectively. The reference frame of map (b) is traveling a the speed of the excited wave, while those of maps (c) and (d) are slower and faster that the excited wave. The map (c) shows the excitation of the gateway mode with wavelength 10.4 nm while plot (d) shows that during dissipation a mode with wavelength 7 nm. nm becomes excited.*

with velocities of 3330 and 8330 ms^{-1}, respectively. It can be clearly seen that the 10.4 nm and 7 nm traveling waves were excited during dissipation.

Movies of both the standing and traveling wave showed that there is some rotation of flexural vibration with an excitation that starts with pure y displacement transferring energy to the degenerate flexural mode with displacement along the x direction. To account for this, all the plots of the mode energy include the energy in all degenerate modes.

It is clear from the plots in Fig.2 that the quality factor during attenuation was not unique. To quantify and compare the dissipation in the tubes as a function of the temperature, the Q factor

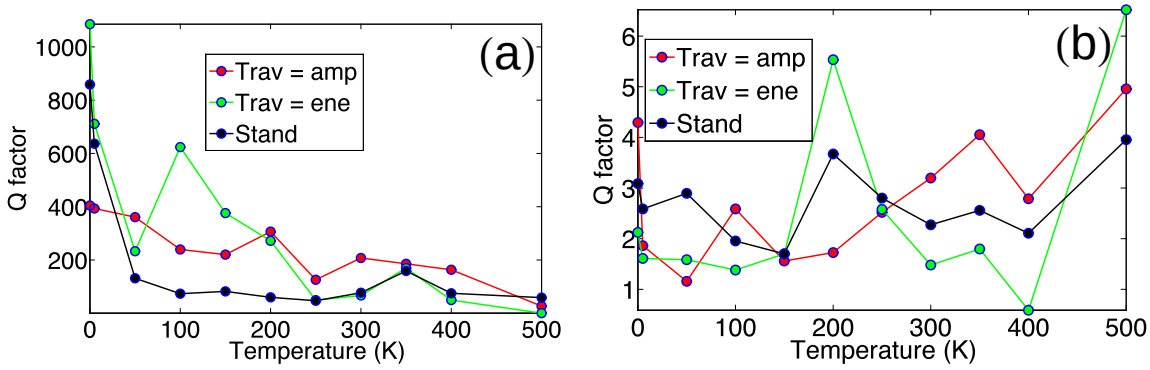

Figure 4: *Q factor as a function of background temperature over the range T_b = 0–500 K. Plot (a) shows Q measured from the initial slope of the ring-down profile, while (c) shows Q measured during the steepest portion of the anomalous dissipation region.*

was computed during two different regions of the dissipation. The initial quality factor, Q_i, was determined from a fit to the initial slope of the ringdown profile (before anomalous dissipation), and is plotted in Fig.4(a). The anomalous quality factor, Q_a, was determined by fitting to the slope of the steepest part of attenuation curve and is plotted in Fig.4(b). The plot of initial quality factor shows that Q_i decreases with increasing T_b as one might expect, while during the anomalous dissipation Q_a is relatively insensitive to the temperature (at least within the accuracy with which we can compute it).

4 Dissipation of a lone traveling wave packet

A wave packet was constructed from traveling flexural modes centered around the 4.2 nm mode (*i.e.* one twentieth of the entire tube). The wave packet had a width of 400 Åand the waveform is shown in Fig.5(a). (The maximum amplitude of the wave packet was 0.4956 Å, which was 4% smaller than that of the largest standing wave. This wave packet contained more than 1000 phonons of energy). The wave packet contained a significant proportion of modes 18–22, and so the energy in the wave packet was computed as the sum of the energy in these five flexural modes. The dissipation of this energy is shown in Fig.5(b). Unlike delocalized standing and traveling waves, the ring-down of wave packets did not exhibit anomalous or delayed dissipation. The attenuation of the wave packet progressed through two distinct phases of dissipation. In the first linear phase, 31% of its initial excitation energy dissipated in 80 picoseconds. Shearing the kinetic energy map into the traveling reference frame (as shown in Fig.5(c)), reveals that the group (envelope) velocity of the wave packet during this period was 9550 ms^{-1}, consistent with the slope of the dispersion relation in Fig.1. This was about 1.5 times faster than the velocity of the central mode and is due to the concave shape of the flexural branch of the dispersion relation. The concave dispersion arises as the shape of the flexural modes crossover from being string-like at long wavelengths to beam-like at shorter wavelengths. Interestingly the velocity of the internal waveform of the wave packet was 8760 ms^{-1} which is slightly slower than the central mode.

After linear dissipation for about 60 ps the wave packet shifted down in frequency and underwent a concomitant reduction in velocity. This marked the beginning of a period with weaker attenuation, overlaid with a long period undulation in the wave packets energy. Shearing the kinetic energy map

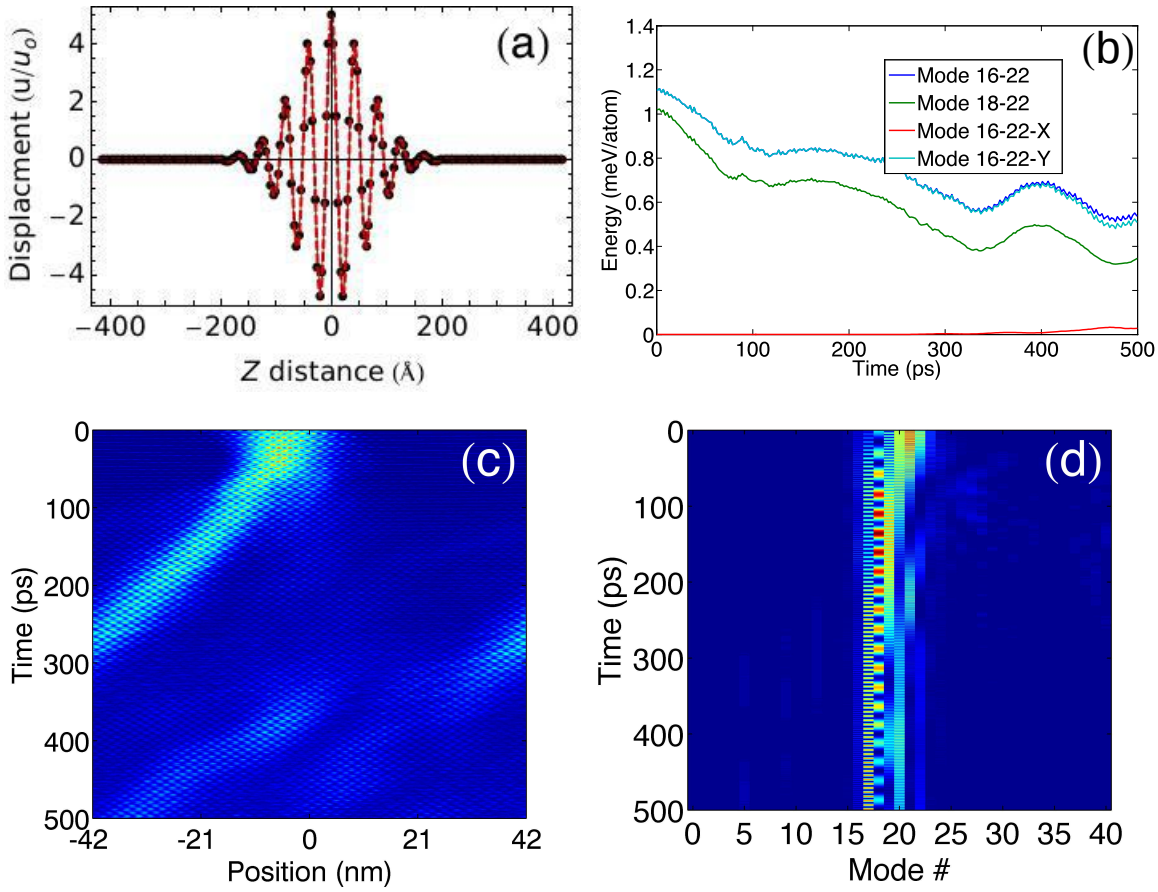

Figure 5: *Plot (a) shows the shape of the wave packets displacement (in dimensionless units). Plot (b) shows the attenuation of energy from the flexural modes 18-22 that comprise the wavepacket, and the total energy in potential low frequency gateway modes (6-10). It can be seen that there is no anomalously rapid or gateway-mode–activated dissipation. Panel (c) maps the kinetic energy along the tube during one simulation. The wave packet is traveling from left to right, and the plot has been sheared into the traveling reference frame. Image (d) maps the flexural mode excitation during the simulation. This is computed from the instantaneous power spectral density of the kinetic energy distribution along the tubes axis. From panels (c & d) it can be seen that after approximately 60 ps the wave packet undergoes a change in its spectral make-up that is accompanied by a reduction in its velocity.*

revealed the reduced velocity to be 790 ms^{-1}. At the beginning of the region the energy dissipated earlier could be seen to spread into higher frequency modes (Fig.5 (d)). It is interesting to note that the wave packet shifted to being centered around mode 18 (a wavelength one 18^{th} of the box) which coincided with the inflection in the dispersion curve. After the down-shift in frequency and velocity the wave packet maintained its average shape, but there was a great deal of structure within the packet, with exchange or beating of energy in the modes that it was composed of. If the energy exchange was a result of beating then measuring the beat frequency, ω_{beat}, gives two possibilities for the frequency, ω_{h}, of the other (hidden) mode participating in the energy exchange, $\omega_{\mathrm{h}} = \omega \pm \omega_{\mathrm{beat}}$. Performing this analysis it was found that the hidden modes did not correspond to the frequencies of the flexural modes and thus it was concluded that this energy exchange is not a result of beating. This should be expected as the modes are orthogonal and so the only coupling between modes is

anharmonic. Simulation of anharmonically coupled pairs of orthogonal modes were performed, but were unable to replicate the energy exchange process. Only by simulating triples of oscillators could the qualitative slow energy exchange behavior be reproduced. In these simulations the inclusion of three mode coupling (*i.e.*, softening of one mode due to the displacement of both other modes) was found to be particularly important for creating large amplitude cycling of energy between oscillators. Thus, it is concluded that the exchange of energy between the modes that make up the wave packet is due to that anharmonic interplay of the multiple modes, and we speculate that this cycling of energy within the wave packet results in a relatively stable phase space trajectory as compared to the standing and traveling waves. One feature that is noticeable by is its absence in Fig.s5(b & c) is the excitation of gateway modes.

At around 300 ps the kinetic energy map showed the wave packet dissolve and reform some distance along the tube. However, this event has no corresponding features in Fig.s5(b & d). When interpreting the kinetic energy map one must remember that the map is sheared into the traveling frame of reference. In this scheme a short pause in the propagation of the wave packet would give the appearance that kinetic energy had teleported along the tube.

Comparing the dissipation of the wave packet with the standing and traveling waves gives several points that are noteworthy: (1) The traveling waves dissipated ∼94% of their energy over the 100 ps simulated while wave packets *with the same amplitude* lost ∼71% of their energy over 500 ps. While both of these vibrations had the same wavelength and the same maximum displacement, the energies were different. The traveling wave is delocalized and so its energy is an extensive property, while the wave packets energy is independent of the tube length. (2) Comparing the wave/wave packet energy and flux in the CNT, we can determine the fraction of dissipation that is thermally resistive. For the traveling wave, all of the dissipation before and after the anomalous region is resistive (*i.e.*, it dissipates into flexural and non-flexural modes with an unbiased choice of wave direction). During the anomalous regime approximately $\frac{1}{3}$–$\frac{1}{2}$ of the energy goes into modes that are also flexural modes with the same direction of travel. Summing the energy in all of the low frequency modes correlates well with the total heat current, indicating that this dissipation does not impact the heat flux and thus is not thermally resistive. For the lone wave packet, the attenuation of the heat flux lags a little behind the dissipation of energy from the flexural modes, at least initially. This indicates that as energy is dissipated from flexural modes it is more likely to transfer to other modes traveling in the same direction.

5 Collisions of flexural wave packets

To further test if gateway modes play a part in the dissipation of wave packets, simulations were performed in which the traveling wave packets were collided with a small displacement gateway wave packet. That is, a second wave packet with wavelength of 10.5 nm and displacement equal to that excited in the gateway mode in Fig.2(d). Three cases were simulated: wave packets initially coincident and traveling in same direction (but with different group velocities); wave packets initially apart and traveling in opposite directions; and wave packets also initially separated but traveling in the same direction. We will refer to these three cases as *center*, *opposite*, and *same* in the figures and discussion that follows.

The attenuation of the energy in the wave packets is plotted in Fig.7. In all cases the presence of the gateway wave packet increased the rate of dissipation from the excited flexural wave packet. The two wave packets had significantly different group velocities of 9550 ms^{-1} and 8760 ms^{-1}. This

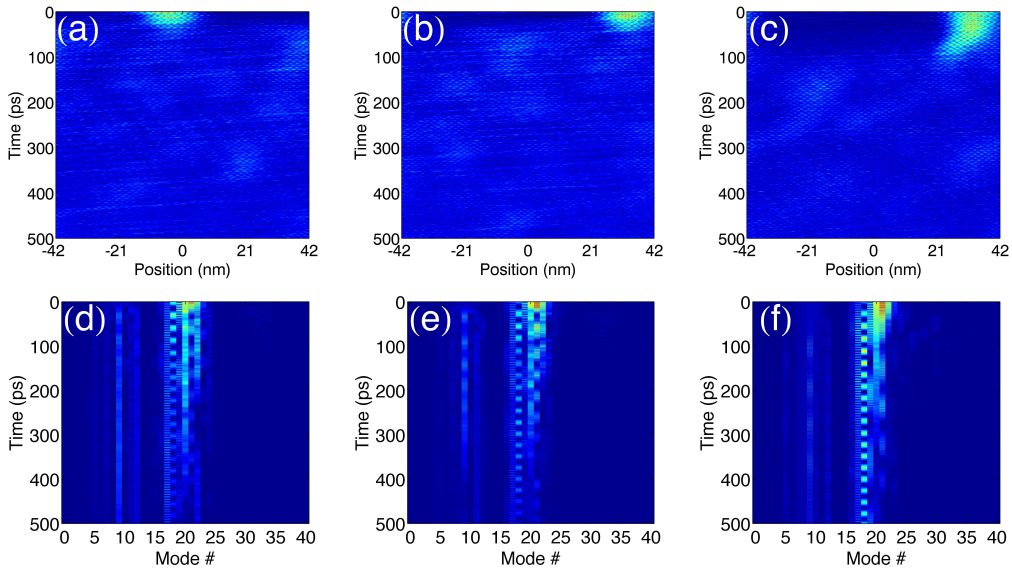

Figure 6: *Kinetic energy distribution maps for collision between wave flexural wave packets. The second colliding gateway mode wave packet is sufficiently low in energy in comparison to the principle wave packet that it cannot be resolved in the maps. Panels (a–c), map the kinetic energy spatially, while panels (d–f) map the energy in k-space. Maps (a & d) are for the* center *configuration, maps (b & e) are for the* same *configuration, and maps (c & f) are for the* opposite *configuration. See text for the description of these different configurations.*

means that the two wave packets collide with each other approximately every 30.4 ps if they are traveling in the same direction, and are 20 ps if they were traveling in opposite directions. In both cases, as the wavepackets collide many times during these simulations the wave packets would be coincident for the same average amount of time. These simulations revealed two surprising result: First, the gateway wave packet accumulated energy as the principle wave packet dissipated. And second, the strength of the dissipation appears to depend on the direction of collision of the wave packets, with co-directional collisions being more dissipative. This implies that in cases of large thermal gradient the thermal conductivity should go down with increasing gradient.

6 Conclusions

It was proposed that anomalous dissipation of flexural vibrations in carbon nanotubes could be exploited for nanomechanical signal processing, permitting the transmission of a signal wave to be turned on or off by the presence of a second gateway signal. A second proposed application was as a thermal switch. In this application the transport of heat through a short nanotube separating two thermal reservoirs would be strongly dependent on the vibrational spectrum of the reservoirs. The motivation for the present work was to determine if anomalous dissipation that was previously observed in standing flexural waves in short nanotubes is also exhibited by longer tubes (which are experimentally more realistic), and also if the same behavior is seen in traveling waves and wave packets.

We found that previously reported anomalous dissipation that is triggered by excitation of special

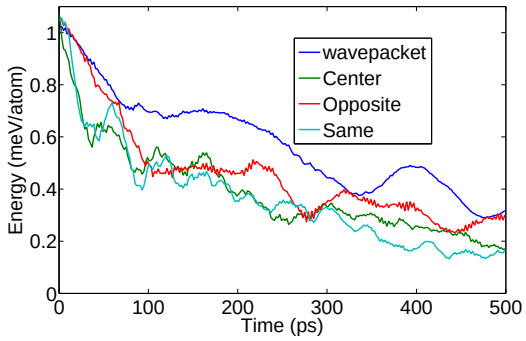

Figure 7: *Attenuation profile of energy in the traveling wave packets while interacting with a gateway wave packet. See text for full description of the* center*,* opposite*, and* same *configurations.*

gateway modes also occurs in these longer tubes. However, anomalous dissipation was not observed during the attenuation of traveling wave packets. It was shown that the dissipation of energy into flexural modes has little effect on the net energy flux while energy dissipated into non-flexural modes is thermally resistive. Finally it was shown that while dissipation of 4.2 nm wavelength wave packets does not display anomalous dissipation, its attenuation is made stronger by collision with a gateway wave packet. Surprisingly, the strength of collision based attenuation is sensitive to the relative direction of the collision.

Together these results support the concept of using nanotubes for nanomechanical signal processing, but do not indicate that the anomalous dissipation effect could be used to make a thermal switch. Instead, the simulation results indicate temperature gradient dependence of the thermal conductivity of a nanotube which might be exploited in a smart thermal device.

7 Acknowledgements

This work used the Extreme Science and Engineering Discovery Environment (XSEDE), which is supported by National Science Foundation grant number OCI-1053575.

References

[1] Rodney S. Ruoff and Donald C. Lorents. Mechanical and thermal properties of carbon nanotubes. *Carbon*, 33(7):925–930, 1995.

[2] Min-Feng Yu. Fundamental mechanical properties of carbon nanotubes: Current understanding and the related experimental studies. *Journal of Engineering Materials and Technology*, 126(3):271, 2004.

[3] Q. W. Li, Y. Li, X. F. Zhang, S. B. Chikkannanavar, Y. H. Zhao, A. M. Dangelewicz, L. X. Zheng, S. K. Doorn, Q. X. Jia, D. E. Peterson, P. N. Arendt, and Y. T. Zhu. Structure-dependent electrical properties of carbon nanotube fibers. *Advanced Materials*, 19(20):33583363, 2007.

[4] J. Hone, M. C. Llaguno, M. J. Biercuk, A. T. Johnson, B. Batlogg, Z. Benes, and J. E. Fischer. Thermal properties of carbon nanotubes and nanotube-based materials. *Applied Physics A*, 74(3):339–343, March 2002.

[5] S. T. Purcell, P. Vincent, C. Journet, and Vu Thien Binh. Tuning of nanotube mechanical resonances by electric field pulling. *Physical Review Letters*, 89(27):276103, December 2002.

[6] Chunyu Li and Tsu-Wei Chou. Single-walled carbon nanotubes as ultrahigh frequency nanomechanical resonators. *Physical Review B*, 68(7):073405, August 2003.

[7] Vera Sazonova, Yuval Yaish, Hande Ustunel, David Roundy, Tomas A. Arias, and Paul L. McEuen. A tunable carbon nanotube electromechanical oscillator. *arXiv:cond-mat/0409407*, September 2004. Nature 431, 284-287, 2004.

[8] H. B. Peng, C. W. Chang, S. Aloni, T. D. Yuzvinsky, and A. Zettl. Ultrahigh frequency nanotube resonators. *Physical Review Letters*, 97(8):087203, August 2006.

[9] Andreas K. Huttel, Gary A. Steele, Benoit Witkamp, Menno Poot, Leo P. Kouwenhoven, and Herre S. J. van der Zant. Carbon nanotubes as ultrahigh quality factor mechanical resonators. *Nano Letters*, 9(7):2547–2552, July 2009.

[10] Chunyu Li and Tsu-Wei Chou. Mass detection using carbon nanotube-based nanomechanical resonators. *Applied Physics Letters*, 84(25):5246–5248, June 2004.

[11] P. Alex Greaney, Giovanna Lani, Giancarlo Cicero, and Jeffrey C. Grossman. Anomalous dissipation in single-walled carbon nanotube resonators. *Nano Letters*, 9(11):3699–3703, November 2009.

[12] P. Alex Greaney, Giovanna Lani, Giancarlo Cicero, and Jeffrey C. Grossman. Mpemba-like behavior in carbon nanotube resonators. *Metallurgical and Materials Transactions A*, 42:3907–3912, 12/2011 2011.

[13] Steven J. Stuart, Alan B. Tutein, and Judith A. Harrison. A reactive potential for hydrocarbons with intermolecular interactions. *The Journal of Chemical Physics*, 112(14):6472–6486, April 2000.

[14] Steve Plimpton. Fast parallel algorithms for short-range molecular dynamics. *Journal of Computaional Physics*, 117:1–19, 1995. `http://lammps.sandia.gov`.

[15] Steven J. Stuart, Alan B. Tutein, and Judith A. Harrison. A reactive potential for hydrocarbons with intermolecular interactions. *The Journal of Chemical Physics*, 112(14):6472–6486, 2000.